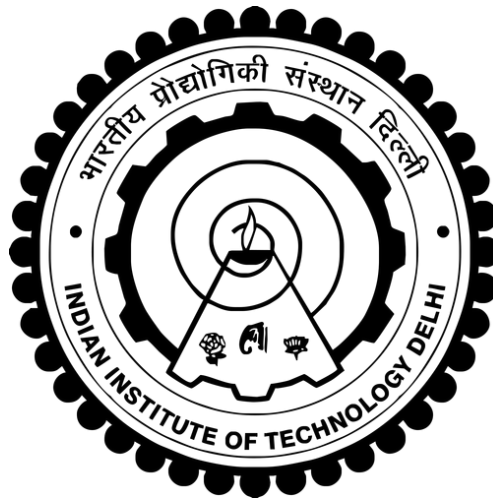


Capacitor-Centric Approaches for Size Reduction and Efficiency Improvement in Electric Vehicle Chargers

Muhammad Zarkab Farooqi



Department of Electrical Engineering
Indian Institute of Technology Delhi

June 2025

© Indian Institute of Technology Delhi (IITD), New Delhi, 2025

Capacitor-Centric Approaches for Size Reduction and Efficiency Improvement in Electric Vehicle Chargers

submitted by

Muhammad Zarkab Farooqi

2018EEZ8566

under the guidance of

Prof. Bhim Singh

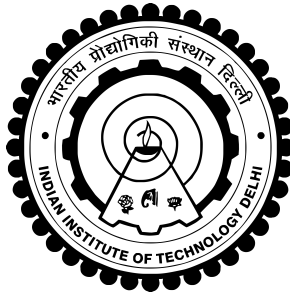
Prof. Bijaya Ketan Panigrahi

Indian Institute of Technology Delhi

for the award of the degree

of

Doctor of Philosophy



**Department Of Electrical Engineering
INDIAN INSTITUTE OF TECHNOLOGY DELHI**

June 2025

THESIS CERTIFICATE

This is to certify that the thesis titled **Capacitor-Centric Approaches for Size Reduction and Efficiency Improvement in Electric Vehicle Chargers**, submitted by **Muhammad Zarkab Farooqi (2018EEZ8566)**, to the Indian Institute of Technology, Delhi, for the award of the degree of **Doctor of Philosophy**, is a bona fide record of the research work done by him under our supervision. The contents of this thesis, in full or in parts, have not been submitted to any other Institute or University for the award of any degree or diploma.

Prof. Bhim Singh

Professor

Dept. of Electrical Engineering
IIT-Delhi, 110016

Place: New Delhi

Prof. Bijaya Ketan Panigrahi

Professor

Dept. of Electrical Engineering
IIT-Delhi, 110016

Place: New Delhi

Date: 30th June 2025

ACKNOWLEDGEMENTS

I would like to extend my heartfelt gratitude to my supervisor, **Prof. Bhim Singh**, and co-supervisor, **Prof. B.K. Panigrahi**, for their unwavering guidance, support, and encouragement. **Prof. Bhim Singh** has been more than just an inspiration; he has been a visionary mentor and a source of strength throughout my doctoral journey. His creativity and dedication to research have continually motivated me, and his influence will guide my career for years to come. Working under his supervision has been an exhilarating experience, allowing me to witness his dedication and passion firsthand. Both **Prof. Bhim Singh** and **Prof. B.K. Panigrahi** have imparted invaluable lessons on discipline, perseverance, and resilience, as well as shared numerous technical insights and ideas. It has been a true privilege to learn from them, be part of their research team, and contribute to the legacy they have built. I am deeply grateful for their trust in me, their teachings, and their continued support.

I would like to extend my sincere gratitude to my SRC members, **Prof. Sumit Pramanick**, **Prof. S. S. Nag**, **Prof. Santanu Kumar Mishra**, and **Prof. T. C. Kandpal**, for their valuable insights, consistent guidance, and constructive feedback, all of which have been instrumental in shaping this thesis.

I am grateful to Prof. Bhim Singh for his financial support for my experiments at IIT Delhi, as well as for covering conference registration and article processing fees. I would also like to extend my sincere thanks to the lab staff—Mr. Puran Singh, Mr. Amit Kumar, Mr. Anurag Singh, and Mr. Jitender Singh—for their invaluable assistance in facilitating my work at the PG Machines Lab, IIT Delhi. I would also like to express my gratitude to my B.Tech supervisor, Prof. Tabish Nazir Mir, for her guidance and support during my B.Tech years, which ultimately paved the way for me to pursue a Ph.D. at IIT Delhi.

Special thanks to my IIT Delhi labmates with whom I had a great experience: Dr. Rohit Kumar, Mrs. Kripa Tiwari, Mr. Sukrashis Sarkar, Ms. Farha Siddique, Ms. Smita Mohanty, Mr. Chetan Shashank Matwankar, Mr. Adnan Farooq Khan, Mr. Arjun Kumar, Mr. Himansu Sahoo, and Mr. Nishant Kumar Singh. I also had the pleasure of working alongside my seniors and juniors, including Dr. Anjeet Verma, Dr. Piyus Kant, Dr. Anshul

Varshney, Dr. Souvik Das, Dr. Gaurav Modi, Dr. Utsav Sharma, Dr. Shalvi Tyagi, Mr. Sandeep Sahoo, Dr. Sudip Bhattacharya, Dr. Syed Bilal Qaiser Naqvi, Dr. Jitendra Gupta, Mr. Gurmeet, Dr. Debasish Mishra, Dr. Aryadip Sen, Dr. Yalavarthi Amarnath, Dr. Hina Parveen, Dr. Rashmi Rai, Dr. Yashi Singh, Dr. Sayandev Ghosh, Dr. Saran Chaurasiya, Dr. Vivek Narayanan, Dr. Suri Rama Naga Praneeth, Dr. Priyvratt Vats, Mr. Rahul Kumar, Mr. Sharankumar Shastri, Mr. Deepak Saw, Dr. Shivam Kumar Yadav, Mrs. Kousalya V, Ms. Sanjenbam Chandrakala Devi, Mr. Junaid Khan, Dr. Subir Karmakar, Mr. Saurabh Mishra, Mr. Vipin Kumar Singh, Mr. Madan Gopal Sharma, Mr. Biswajit Saha, Mr. Sumit Kumar, Mr. Gaurav Kumar, Mr. Siddharth Ghosh, Mr. Praveen Kumar Singh, Mr. Suvom Roy, Mr. Subhadip Chakraborty, Mr. Qayamuddin, Mr. Abhrodip Chaudhury, Mr. Akash Kedia, Mr. Purusharth Semwal, Mr. Abhishek Abhinav Nanda, Mr. Aswin Dilip Kumar, Mrs. Sunaina Singh, and all members of the PG Machines lab for their invaluable support.

I am grateful to my roommates at Nilgiri Hostel, Mr. Danish Nissar, Dr. Nadeem Beigh, and Dr. Omais Shafi, whose constant support made my PhD journey much easier. I would also like to sincerely thank all my friends: Mr. Jasir Arafat, Dr. Aamir Rafiq, Dr. Saleem Mir, Mr. Adnan Farooq, Mr. M. Saleh Khan, Mr. Rafiq, Mr. Umer Ali, Mr. Faiz Masood, Mr. Saqib Abbas, Mr. Mujeeb, Mr. Faizan Beigh, Mr. Mustansir, and Mr. Adil Bashir, for their companionship and encouragement throughout this time.

I am deeply grateful to the loving and supportive figures in my life, my mother, Mrs. Nahida Farooqi, and my father, Mr. Zahoor Ahmad Farooqi. Their unwavering encouragement has been instrumental in making this journey possible. I also extend my heartfelt thanks to my brother, Mr. Mohammad Zakariya Farooqi, for his constant support and affection. I would also like to thank my fiancée, Ms. Aroosa Khan, for her support.

Finally, I want to thank the Almighty for granting me the strength and patience to navigate all of life's ups and downs.

Date: 30th June 2025

Muhammad Zarkab Farooqi

ABSTRACT

Power electronics play a crucial role in industrial applications, with electric vehicles (EVs) being one of the most prominent examples. EVs rely on battery chargers to replenish their battery packs, making features like efficiency, high power density, and reliability essential in such systems. Traditional grid-connected EV chargers typically use an AC-DC-DC architecture. However, this design often involves bulky electrolytic capacitors in single-phase converter systems, contributing to a larger overall footprint. A promising alternative to these capacitors is the use of active power buffers (APBs). APB converters enable the use of low-capacitance DC-port capacitors by either transferring the ripple from the DC port to another component within the circuit or by generating a counter-ripple waveform to cancel it out. These converters offer significant advantages, such as enhanced power density, improved reliability, and better input/output power quality. Due to these benefits, APBs were prominently utilised by participants in the Google Little Box Challenge, an industry-level competition aimed at advancing the power density of AC-DC converters.

Although APBs offer several advantages, their industrial application has been limited. This is mainly due to the considerable efficiency loss compared to passive solutions, the increased system complexity from adding switches and sensors, and their lack of robustness. While some challenges have been addressed through research, others remain under investigation, particularly regarding their practical implementation. This thesis focuses on the design and development of converters and techniques aimed at reducing capacitor requirements in single-phase and single-phase-derived converters. It presents novel and enhanced modulation and control strategies for APB converters, with a focus on improving performance and reducing complexity. To minimize ripple at the load end while using low-value capacitance, two types of APB topologies are examined: non-integrated and integrated APBs. The unique challenges of each category are addressed, and their suitability for EV chargers is analyzed in this thesis.

Non-integrated APBs are commonly explored topologies for reducing capacitor ripple in AC-DC systems due to their independent control and plug-and-play operation. Based on their power processing capabilities, non-integrated APBs can be further classified into two categories: complete-power processing APBs and partial-power processing APBs. Complete-

power processing APBs, which are most commonly used, tend to have higher efficiency drop. Many researchers have proposed control and modulation techniques to improve the efficiency of these APBs, bringing their losses closer to those of passive solutions, such as electrolytic capacitors (E-caps). Although operating these APB converter in a critical-conduction mode can reduce switching losses, this technique is not beneficial at high power levels. This thesis addresses enhanced modulation and control strategies for complete-power processing APBs, aimed at further improving efficiency across a wide range of operating conditions and optimizing performance during dynamic periods. Furthermore, partial-power processing APB converters, which exhibit efficiency comparable to passive solutions, have the drawback of an increased sensor count. This issue is tackled by introducing an adaptive non-linear control strategy to reduce reliance on sensors, thereby enhancing reliability and reducing system complexity. All modulation techniques and control algorithms are developed in the MATLAB/Simulink environment, followed by magnetic and thermal simulation validation in COMSOL Multiphysics. Finally, experimental verification is conducted on various two-layer PCB prototypes of different APB converters, as well as a conventional front-end AC-DC converter, using the Texas Instruments TMS320F28379D microcontroller.

To enable power decoupling with minimal or no additional semiconductor switches, the adoption of integrated APB converters has been proposed in the literature. These converters have gained attention in the research community in recent years due to their reduced cost and lower system complexity. This thesis also investigates the potential of integrating a secondary-stage DC-DC converter with the APB, thereby maintaining the front-end H-bridge-based AC-DC converter structure and paving the way for the use of integrated APBs in multilevel converters. Furthermore, the thesis explores the possibility of repurposing the decoupling circuitry of integrated APBs to add multifunctional capabilities in EVs. The integrated APB converters are first validated conceptually through simulations in MATLAB/Simulink and Ansys MAXWELL, followed by experimental verification using SiC MOSFET-based hardware prototypes.

सारांश

पावर इलेक्ट्रॉनिक्स औद्योगिक अनुप्रयोगों में एक महत्वपूर्ण भूमिका निभाता है, जिसमें इलेक्ट्रिक वाहन (EVs) को सबसे प्रमुख उदाहरणों में से एक माना जाता है। EVs अपनी बैटरी पैक्स को फरि से चार्ज करने के लिए बैटरी चार्जर पर निर्भर करते हैं, जिससे इस प्रकार के सिस्टम में दक्षता, उच्च पावर डेंसिटी और विश्वसनीयता जैसी विशेषताएँ आवश्यक हो जाती हैं। पारंपरिक ग्रिड-के कनेक्टेड EV चार्जर सामान्यतः एक AC-DC-DC आर्किटेक्चर का उपयोग करते हैं। हालांकि, यह डिज़ाइन अक्सर सगिल-फेज कन्वर्टर सिस्टम में भारी इलेक्ट्रोलाइटिक कैपेसिटर्स का उपयोग करता है, जो पूरे सिस्टम का आकार बढ़ाने में योगदान करता है। इन कैपेसिटर्स के एक आशाजनक विकल्प के रूप में सक्रिय पावर बफर्स (APBs) का उपयोग किया जा सकता है। APB कन्वर्टर, DC पोर्ट कैपेसिटर्स के लिए कम कैपेसिटंस का उपयोग करने की अनुमति देते हैं, या तो DC पोर्ट से रपिल को सर्किट के किसी अन्य घटक में ट्रांसफर करके, या एक काउंटर-रपिल वेवफॉर्म जनरेट करके इसे रद्द करने के द्वारा। ये कन्वर्टर महत्वपूर्ण लाभ प्रदान करते हैं, जैसे कि बेहतर पावर डेंसिटी, बेहतर विश्वसनीयता और बेहतर इनपुट/आउटपुट पावर क्वालिटी। इन लाभों के कारण, APBs का प्रमुख रूप से उपयोग किया गया था गूगल लटिलि बॉक्स चैलेंज में, जो एक उद्योग-स्तरीय प्रतियोगिता है जिसका उद्देश्य AC-DC कन्वर्टर की पावर डेंसिटी को बढ़ाना है।

हालांकि APBs कई लाभ प्रदान करते हैं, उनके औद्योगिक अनुप्रयोग सीमित रहे हैं। इसका मुख्य कारण यह है कि वे पासवि समाधानों की तुलना में काफी दक्षता हानि करते हैं, स्वचिस और सेंसर जोड़ने से सिस्टम की जटिलता बढ़ जाती है, और उनकी मजबूतता की कमी होती है। जबकि कुछ चुनौतियों को शोध के माध्यम से हल किया गया है, अन्य अभी भी जांच के अधीन हैं, विशेष रूप से उनके व्यावहारिक कार्यान्वयन के संबंध में। यह शोध सगिल-फेज और सगिल-फेज-व्युत्पन्न कन्वर्टर में कैपेसिटर्स की आवश्यकता को कम करने के लिए डिज़ाइन और तकनीकों के विकास पर केंद्रित है। यह APB कन्वर्टर के लिए नवीन और उन्नत मॉड्यूलन और नियंत्रण रणनीतियाँ प्रस्तुत करता है, जिनका उद्देश्य प्रदर्शन को सुधारना और जटिलता को कम करना है। लोड के अंत पर रपिल को कम करने के लिए और कम मूल्य वाले कैपेसिटर्स का उपयोग करते हुए, दो प्रकार की APB टॉपोलॉजीज की जांच की जाती है: नॉन-इंटीग्रेटेड और इंटीग्रेटेड APBs। प्रत्येक श्रेणी की विशिष्ट चुनौतियों को संबोधित किया जाता है, और EV चार्जर के संदर्भ में उनकी उपयुक्तता का विश्लेषण किया जाता है।

नॉन-इंटीग्रेटेड APB कन्वर्टर को AC-DC सिस्टम में कैपेसिटर्स रपिल को कम करने के लिए सामान्यतः अन्वेषित टॉपोलॉजीज माना जाता है, क्योंकि इनमें स्वतंत्र नियंत्रण और प्लग-एंड-प्ले ऑपरेशन होता है। इनके पावर प्रोसेसिंग क्षमताओं के आधार पर, नॉन-इंटीग्रेटेड APBs को दो श्रेणियों में और विभाजित किया जा सकता है: पूर्ण-पावर प्रोसेसिंग APBs और आंशिक-पावर प्रोसेसिंग APBs। पूर्ण-पावर प्रोसेसिंग APBs, जो सामान्यतः उपयोग किए जाते हैं, उच्च कन्वर्टर हानि के लिए प्रवृत्त होते हैं। कई शोधकर्ताओं ने इन APBs की दक्षता को सुधारने के लिए नियंत्रण और मॉड्यूलन तकनीकों का प्रस्ताव किया है, जिससे उनकी हानियाँ पासवि समाधानों, जैसे कि इलेक्ट्रोलाइटिक कैपेसिटर्स (E-caps), के समान हो जाती हैं। हालांकि,

कन्वर्टर को क्रिटिकल-कंडक्शन मोड में चलाने से स्वचिगि हानियों को कम किया जा सकता है, यह तकनीक उच्च पावर स्तरों पर लाभकारी नहीं होती है। यह शोध पूर्ण-पावर प्रोसेसिंग APBs के लिए उन्नत मॉड्यूलन और नियंत्रण रणनीतियों को संबोधित करता है, जिनका उद्देश्य ऑपरेटिंग स्थितियों की वसित श्रृंखला में दक्षता को और सुधारना और गतिशील अवधियों के दौरान प्रदर्शन को अनुकूलित करना है। इसके अलावा, आंशिक-पावर प्रोसेसिंग APB कन्वर्टर्स, जो पैसवि समाधानों के समान दक्षता प्रदर्शित करते हैं, उनके पास एक अतिरिक्त सेंसर की आवश्यकता का नुकसान होता है। यह शोध इस समस्या का समाधान एक अनुकूलनशील नॉन-लिनियर नियंत्रण रणनीति द्वारा करता है, जो सेंसर पर निर्भरता को कम करता है, इस प्रकार विश्वसनीयता को बढ़ाता है और सिस्टम की जटिलता को घटाता है। सभी मॉड्यूलन तकनीकों और नियंत्रण एल्गोरिदम MATLAB/Simulink वातावरण में विकसित की जाती हैं, इसके बाद COMSOL Multiphysics में मैग्नेटिक और थर्मल सिमुलेशन स्थापित किया जाता है। अंत में, विभिन्न APB कन्वर्टर्स के विभिन्न दो-परत पीसीबी प्रोटोटाइपों पर और एक पारंपरिक फ्रंट-एंड AC-DC कन्वर्टर पर, Texas Instruments TMS320F28379D माइक्रोकंट्रोलर का उपयोग करके प्रयोगात्मक स्थापित किया जाता है।

पावर डिकिपलिंग को सक्षम बनाने के लिए न्यूनतम या बिना अतिरिक्त सेमीकंडक्टर स्वचि के, एकीकृत APB कन्वर्टर्स को अपनाने का प्रस्ताव दिया गया है। इन कन्वर्टर्स ने हाल के वर्षों में अपनी कम लागत और कम सिस्टम जटिलता के कारण शोध समुदाय में ध्यान आकर्षित किया है। इस शोध में APB के साथ एक द्वितीयक-चरण DC-DC कन्वर्टर को एकीकृत करने की संभावना की भी जांच की गई है, ताकि फ्रंट-एंड H-ब्रिज आधारित AC-DC कन्वर्टर संरचना बनाए रखते हुए, एकीकृत APBs को मल्टीलेवल कन्वर्टर्स में उपयोग के लिए मार्ग प्रशस्त किया जा सके। इसके अलावा, यह कार्य एकीकृत APBs के डिकिपलिंग सर्किटरी का पुनः उपयोग करने की संभावना का अन्वेषण करता है ताकि EVs में बहु-कार्यात्मक क्षमताएँ जोड़ी जा सकें। एकीकृत APB कन्वर्टर्स को पहले MATLAB/Simulink और Ansys MAXWELL में सिमुलेशन के माध्यम से अवधारणात्मक रूप से स्थापित किया जाता है, और फिर SiC MOSFET-आधारित हार्डवेयर प्रोटोटाइप का उपयोग करके प्रयोगात्मक स्थापित किया जाता है।

Contents

THESIS CERTIFICATE	i
ACKNOWLEDGEMENTS	ii
ABSTRACT	iv
LIST OF FIGURES	xix
LIST OF TABLES	xx
ABBREVIATIONS	xxi
NOMENCLATURE	xxiii
CHAPTER 1 INTRODUCTION	1
1.1 General	1
1.2 Discussion on Capacitive-Centric Methods for AC-DC Converters	4
1.2.1 Control Technique for Second-Order Ripple Reduction for AC-DC Converters without additional circuitry	4
1.2.2 State-of-the art Active Power Buffer Circuits for AC-DC Converters	5
1.2.3 Integrated and Multifunctional AC-DC Converters with Active Power Buffering Capability	6
1.2.4 Ripple Reduction in Three-phase Phase-modular and Multilevel AC-DC Converters	6
1.3 Outline of Chapters	7
CHAPTER 2 LITERATURE REVIEW	11
2.1 General	11
2.2 Literature Survey	11
2.2.1 Google-Little Box Challenge	12
2.2.2 Review of Active Power Buffer Converters	12
2.2.2.1 Non-integrated Active Power Buffer Converters	13
2.2.2.2 Integrated Active Power Buffer Converters	15
2.2.3 Review of Control Techniques for Active Power Buffer Converters .	18
2.2.3.1 Injection/ Suppression-based Control	18
2.2.3.2 Ripple Power-Based Control	19
2.2.3.3 Model-based Control	19
2.3 Identified Areas of Research	20
2.4 Objectives and Scope of work	21
2.5 Conclusions	22

CHAPTER 3	POWER CONVERTERS Configurations AND DESIGN FOR AC-DC-DC CONVERSION USING Si-IGBTs AND SiC-MOSFETs	24
3.1	General	24
3.2	Gate Driver and Auxiliary Circuitry for Semiconductor Switches	24
3.3	IGBT-based Power Converters	24
3.4	SiC MOSFETs based Power Converters	25
3.4.1	Design and Layout of Gate Driver Boards	25
3.4.2	Design and Layout of Power Boards	27
3.4.3	Design and Layout of unified current/ voltage and micro-controller board	27
3.5	Execution of Control Algorithm Using TMSF2- 83795D Microcontroller . .	31
3.6	Various Hardware Setups	31
3.7	Results and Discussion	33
3.7.1	Test Results with Si-IGBTs of AC-DC Power Converter	34
3.7.2	Test Results with SiC-MOSFETs of AC-DC-DC Power Converter and DESAT Protection Trigger	35
3.8	Conclusions	36
CHAPTER 4	MINIMUM CAPACITOR REQUIREMENT IN SINGLE-PHASE AC-DC CONVERTERS AND FEEDFORWARD METHOD FOR IMPROVED PERFORMANCE	37
4.1	General	37
4.2	Double-line frequency ripple in single-phase half-bridge and full-bridge AC-DC converter	38
4.2.1	Voltages expressions for half-bridge AC-DC converter	39
4.2.2	Voltages expressions for full-bridge AC-DC converter	40
4.3	Minimum Capacitor Requirement in half-bridge and Full-bridge AC-DC Converters	41
4.3.1	Minimum capacitance calculations for half-bridge AC-DC converter	41
4.3.2	Minimum capacitance calculations for full-bridge AC-DC converter	42
4.4	Modified Model Predictive Feedforward Control for Enhanced Dynamic Performance in AC-DC Converters with Low-Value DC-port Capacitance . . .	44
4.4.1	Model Predictive Control	44
4.4.2	Modified MPC with feedforward	45
4.4.3	Stability Analysis	48
4.5	MATLAB-based Modeling and Simulation of front-end Half-bridge and full-bridge AC-DC Converter	48
4.6	Hardware Implementation of full-bridge AC-DC converter operating with modified model predictive control	48
4.7	Results and Discussion	49
4.7.1	Scenario I: Conventional Control without any digital filter	50
4.7.2	Scenario II: Control with BSF, MUT and MPC with K fixed at 1	50
4.7.3	Scenario III: MUT-MPC Control with K dependent on NEV	53
4.8	Conclusions	53

CHAPTER 5	IMPROVED EFFICIENCY WITH HYBRID CCM-CRM MODULATION TECHNIQUE FOR NON-INTEGRATED ACTIVE POWER BUFFERS	55
5.1	General	55
5.2	Discussion on Modulation Strategies for complete power processing-based Active Power Buffer Converter	56
5.3	Operating Principle of complete power processing based Active Power Buffer Converter	57
5.3.1	Modulation Principles for Active Power Buffer Operation	57
5.3.1.1	Continuous Conduction Mode	57
5.3.1.2	Critical Mode Operation (using ZCD)	59
5.3.1.3	ZCD-free Critical Conduction Mode Operation	60
5.4	Loss Analysis of complete power processing-based Active Power Buffer Converter in CCM and CRM (ZCD-free)	60
5.4.1	Conduction Losses	61
5.4.2	Core Losses	62
5.4.3	Switching Losses	63
5.4.4	Winding and ESR Losses	63
5.5	Proposed hybrid CCM-CRM based Modulation Technique for complete power processing ba-sed Active Power Buffer Converter	65
5.5.1	Instantaneous Loss Distribution	65
5.5.2	Optimal efficiency performance with hybrid CCM-CRM	66
5.6	Multi-Objective Optimization Formulation	67
5.6.1	Discussion on Design Variables	67
5.6.2	Optimization Formulation	67
5.6.2.1	Loss Objective Function	67
5.6.2.2	Volume Objective Function	68
5.6.3	Comparative Assessment	69
5.7	Optimal Efficiency-shift Control of complete power processing-based Active Power Buffer Converter with hybrid CCM-CRM Modulation	73
5.8	MATLAB-based Modeling and Simulation of complete power processing Active Power Buffer Converter with hybrid CCM-CRM Modulation	74
5.9	Hardware Implementation of complete power processing-based Active Power Buffer Conve-rter with hybrid CCM-CRM Modulation	75
5.10	Results and Discussion	75
5.10.1	Performance of Active Power Buffer Converter with CCM Modulation	75
5.10.2	Performance of Active Power Buffer Converter with CRM Modulation	76
5.10.3	Performance of Active Power Buffer Converter with hybrid CCM-CRM Modulation	76
5.11	Comparative Discussion based on Efficiency Drop with various Modulation Techniques for complete power processing-based Active Po-wer Buffer Converter	79
5.12	Conclusions	80
CHAPTER 6	Improved Dynamic Performance of CRM operated NON-INTEGRATED Active Power Buffers	82
6.1	General	82
6.2	Analysis and conventional Closed-loop control of buck-based APB circuit	83

6.2.1	Power Ripple Analysis	83
6.2.2	CCM for APB Converter	84
6.3	Critical Conduction Mode Constraints for non-integrated complete power processing-based Active Power Buffer Converter	85
6.4	Active Ripple Elimination for Robust Control and Enhanced Dynamic Performance of CRM-based Active Power Buffer	88
6.4.1	Average Decoupling Capacitor Voltage	88
6.4.2	Active Ripple Elimination	89
6.4.3	Inner Current and Reference Generation Loop	91
6.5	Design Aspect, Analysis and Comparison	91
6.5.1	Small Signal Modelling of non-integrated complete power processing based active power buffer converter	91
6.5.2	Design of Voltage Controller using Small-signal Modelling with Conventional Control	92
6.5.3	Design of Voltage Controller using Small-signal Modelling with Active Ripple Elimination for Robust Control	93
6.6	MATLAB-based Modeling and Simulation of non-integrated complete power processing-based Active Power Buffer Converter with Active Ripple Elimination based Robust Control for Enhanced Dynamic Performance	95
6.7	Hardware Implementation of non-integrated complete power processing-based Active Power Buffer Converter with Active Ripple Elimination-based Robust Control for Enhanced Dynamic Performance	95
6.8	Results and Discussion	96
6.8.1	Simulation Results	96
6.8.2	Experimental Results	97
6.8.2.1	Steady-state Results	97
6.8.2.2	Dynamic Results	97
6.9	Conclusions	101

CHAPTER 7 MULTIFUNCTIONAL INTEGRATED ON-BOARD ELECTRIC VEHICLE CHARGER WITH ACTIVE POWER BUFFERING CAPABILITY 102

7.1	GENERAL	102
7.2	Configurations of Integrated On-Board Electric Vehicle Charger	103
7.2.1	System Description and Analysis	104
7.2.2	Operating Principle in Charging Mode	106
7.2.3	Electromagnetic Torque during G2V and V2G	107
7.3	Design Considerations for Integrated On-Board Electric Vehicle Charger	109
7.3.1	Inductance Variation in PMSM	109
7.3.2	FEM Analysis of PMSM in Charging Mode	111
7.3.3	Current Ripple Variations due to Changing PMSM Winding Inductance	111
7.4	Control and Modulation Strategy for presented integrated APB-based Integrated On-Board Electric Vehicle Charger	112
7.4.1	Improved Control integrated APB-based On-Board Integrated Electric Vehicle Charger	113
7.4.1.1	DC-port Voltage and Input Power Quality Control	113
7.4.1.2	Integrated Active Power Buffering Control	115

7.4.2	Variable Switching Frequency-based PWM	116
7.4.3	EMI with Variable Frequency Modulation	117
7.5	MATLAB-based Modeling and Simulation of Multifunctional APB-based Integrated On-Board Electric Vehicle Charger	117
7.6	Hardware Implementation of Multifunctional integrated APB-based Integrated On-Board Electric Vehicle Charger	117
7.7	Results and Discussion	118
7.7.1	Simulation Results	118
7.7.2	Experimental Results	121
7.7.2.1	Steady-state results of presented charging topology in G2V mode	121
7.7.2.2	Steady-state results of the presented charger in V2G mode	122
7.7.2.3	Dynamic performance of presented charger	123
7.8	Conclusions	123

CHAPTER 8 REDUCED SWITCH COUNT BASED INTEGRATED ISOLATED DC-DC CONVERTER WITH ACTIVE POWER BUFFERING CAPABILITY FOR MULTI-LEVEL CONVERTERS 125

8.1	GENERAL	125
8.2	Configurations for Switch-Count Reduction in Active Power Buffer Converter	126
8.3	DC-port Capacitor Requirements in Multilevel and Phase-Modular Converters	127
8.4	Conceptual Evolution and Working Principle of Half-bridge Isolated Integrated Active Power Buffer Converter	129
8.4.1	Modes of Operation	131
8.4.1.1	Operation in Mode-I	131
8.4.1.2	Operation in Mode-II	131
8.4.1.3	Operation in Mode-III	133
8.4.1.4	Operation in Mode-IV	133
8.4.2	Power Equation and ZVS Constrains	133
8.4.2.1	Active Cases (Case-I and Case-III) Power Equation and ZVS Constrains	133
8.4.2.2	Redundant Cases (Case-II and Case-IV) Power Equation	135
8.5	Control Strategy for Half-bridge Isolated Integrated Active Power Buffer Converter	138
8.5.1	Secondary-stage Isolated Integrated Active Power Buffer Control	138
8.5.2	Front-end CHB and BES Control	140
8.5.3	Capacitor Balancing and SOC Balancing Control	141
8.6	MATLAB-based Modeling and Simulation of Half-bridge Isolated Integrated Active Power Buffer Converter	141
8.7	Hardware Implementation of Half-bridge Isolated Integrated Active Power Buffer Converter	142
8.8	Results and Discussion	142
8.9	Conclusions	145

CHAPTER 9	NON-LINEAR OBSERVER BASED SENSOR REDUC- TION TECHNIQUE FOR Partial-Power Processing based SERIES-STACKED BUFFER	147
9.1	General	147
9.2	Series-stacked buffer and Non-linear Current Observer-based Control . . .	148
9.2.1	Control Objectives of SSB	148
9.2.2	Mathematical Model of SSB	149
9.2.3	Non-Linear Current Observer	150
9.2.4	Calculation of Correction Terms	150
9.2.5	Discrete Expression of Adaptive Non-Linear Current Observer . . .	151
9.2.6	Qualitative Discussion on SSB Capacitor Ripple	152
9.3	SSB Control with Adaptive Non-Linear Current Observer	153
9.4	MATLAB-based Modeling and Simulation of Series-Stacked Buffer with cur- rent sensorless operation	155
9.5	Results and Discussion	155
9.6	Conclusion	160
CHAPTER 10	MAIN CONCLUSIONS AND SUGGESTIONS FOR FUR- THER WORK	162
10.1	General	162
10.2	Main Conclusions and Final Recommendations	163
10.3	Suggestions for Future Work	165
REFERENCES		167
LIST OF PUBLICATIONS		183
BIO-DATA		185

List of Figures

1.1	AC-DC power electronic converters utilized in various applications	2
2.1	(a) Buck-based APB connected at the DC-port, (b) boost-based APB, and (c) buck-boost based APB	14
2.2	(a) Split capacitor arrangement based half-bridge APB converter, (b) Full-bridge based APB converter	14
2.3	Series-stacked buffer converter	15
2.4	(a) Half-bridge integrated APB converter, (b) full-bridge integrated APB converter	16
2.5	(a) Buck-derived integrated APB converter, (b) Boost-derived integrated APB converter	17
2.6	(a) Modified integrated APB converter, (b) Doubly grounded integrated APB converter	17
3.1	Schematic of gate driver circuit (IC-UCC21750) [1]	26
3.2	Two Layer 64mm*69mm PCB design of Gate Drivers (a) Top Layer, and (b) Bottom Layer	26
3.3	RCD Snubber circuits along with decoupling capacitor for single-leg SiC	27
3.4	Circuit diagram of the hardware prototype of three-leg power board	28
3.5	Two Layer 127mm*164mm PCB design of three-leg power board (a) Top Layer, and (b) Bottom Layer	28
3.6	Two Layer 126mm*197mm PCB design of two-leg with split capacitors or SSB capacitors power board (a) Top Layer, and (b) Bottom Layer	28
3.7	Signal conditioning circuit for sensing voltages and currents using LEM sensors	30
3.8	Two Layer 128mm*162mm PCB design of unified sensor and TMS32028379D microcontroller board with (a) Top Layer, and (b) Bottom Layer	30
3.9	DSP code length of $11.52\mu s$ with sampling frequency of $50kHz$	31
3.10	(a) 4-Leg IGBT based converter for AC-DC conversion along with programmable AC source and 120V 24Ahr battery, (b) current/voltage sensors plus microcontroller board	32
3.11	(a) Complete SiC based converter setup for AC-DC power conversion using integrated isolated DC-DC converter, (b) zoomed view of integrated isolated DC-DC converter	33
3.12	SiC based experimental setups for (a) dual-active bridge (DAB), (b) series-stacked buffer (SSB)	34
3.13	Steady-state performance of IGBT-based half-bridge AC-DC converter with split capacitors (V_g : Grid voltage, i_g : Grid current, V_{DC1} , V_{DC2} : Split-capacitor voltages)	34

3.14	Steady-state performance of DAB connected to the front-end AC-DC converter (V_g : Grid voltage, i_g : Grid Current, V_{bat} : Battery voltage, i_{bat} : Battery current, V_{prim} : Primary side transformer voltage, V_{sec} : Secondary side transformer voltage, i_{prim} : Primary side transformer current, i_{sec} : Secondary side transformer current)	35
3.15	Test results of DESAT protection trigger operation of SiC-MOSFETs based active power buffer converter operating with critical conduction mode	35
4.1	Front-end AC-DC converter of (a) half-bridge configuration (b) full-bridge configuration	39
4.2	Capacitor voltage waveforms of half-bridge based AC-DC converter with minimum split-capacitance of $C_{dc1}, C_{dc2} = 180\mu F$	43
4.3	Capacitor voltage and grid voltage waveforms with minimum capacitance	44
4.4	(a) MUT-MPC for front-end AC-DC Converter, (b) VC loop with MUT control, (c) Flowchart of MUT-MPC control	47
4.5	MATLAB simulation block of modified model predictive control for improved dynamic performance in AC-DC converter	49
4.6	Performance of AC-DC converter with conventional control without a digital filter: (a) 200W increase in load (b) 200W decrease in load (c)-(e) Power quality analyzer results at 180W (f)-(h) Power quality analyzer results at 375W	51
4.7	Performance of AC-DC converter with BSF and MUT-MPC Control (K=1 fixed): (a) 200W increase in load (b) 200W decrease in load. Performance of AC-DC with MUT-MPC Control (K is dependent on NEV): (c) 200W increase in load (d) 200W decrease in load (e)-(g) Power quality analyzer results at 180W (h)-(i) Power quality analyzer results at 375W	52
5.1	Buck-based active power buffering circuitry with parasitic switch capacitances and non-idealities	57
5.2	Voltage and current waveforms of APB converter	58
5.3	Time-exaggerated view of APB inductor current waveform within twice-line frequency cycle while operating with hybrid CCM-CRM	66
5.4	Volumetric magnetic flux density plot of HJS301090 (a) Sliced-view, (b) surface-view	69
5.5	Instantaneous loss distribution of buck-type APB operating with (a) CCM at 20% of P_{max} , (b) CCM at 40% of P_{max} , (c) CCM at 60% of P_{max} , (d) CCM at 80% of P_{max} , (e) CCM at 100% of P_{max} , (f) CRM at 20% of P_{max} , (g) CRM at 40% of P_{max} , (h) CRM at 60% of P_{max} , (i) CRM at 80% of P_{max} , (j) CRM at 100% of P_{max}	71
5.6	Exaggerated view of current waveforms during half of twice-line frequency cycle with CCM activated under high instantaneous current I_b whereas CRM selected below critical instantaneous current I_b . $\theta_\alpha - \theta_\beta$ are the critical points of PLL	72
5.7	Temperature density plot of HJS301090 operating with (a) CCM modulation, (b) CRM modulation, and (c) hybrid CCM-CRM modulation	72
5.8	Temperature density plot of UF3C120040K switches with PA-T22-38 heat-sink operating with (a), (b) CCM modulation, (c), (d) CRM modulation, and (e), (f) hybrid CCM-CRM modulation	73

5.9	Overall control diagram of buck-based active power buffer converter operating with hybrid CCM-CRM modulation	74
5.10	MATLAB/ Simulink model of buck-based APB converter connected at DC-port of front-end AC-DC converter with APB operating with proposed hybrid CCM-CRM control and modulation	75
5.11	Experimental results of buck-based APB converter operating with: (a) CCM modulation and control, (b) Zoomed-in view of APB converter waveforms showing hard-switching of M_1 in positive half-cycle of i_b with CCM, (c) Zoomed-in view of APB converter waveforms showing hard-switching of M_2 in negative half-cycle of i_b with CCM.	77
5.12	Experimental results of buck-based APB converter operating with: (q) CRM modulation and control, (b) Zoomed-in view of APB converter waveform showing soft-switching of M_1 in positive half-cycle of i_b with CRM, (c) Zoomed-in view of APB converter waveform showing soft-switching of M_2 in negative half-cycle of i_b with CRM.	77
5.13	Experimental results of buck-based APB converter operating with presented hybrid CCM-CRM modulation and control (a) zoomed-view of switch voltages and i_b transiting from CRM to CCM, (b) zoomed-view of switch voltages and i_b transiting from CCM to CRM, (c) positive-half of i_b with hybrid CCM-CRM, (d) negative-half of i_b with hybrid CCM-CRM, (e)-(f) grid current (i_g) along with APB converter voltages and currents in positive and negative half-cycle of i_b	78
5.14	Experimental results showing buck-based APB converter currents and voltages along with grid current (i_g) operating with presented hybrid CCM-CRM modulation and control at (a) 20% of P_{max} , (b) 40% of P_{max} , (c) 60% of P_{max} , (d) 80% of P_{max} , (e) 100% of P_{max}	79
5.15	Power quality analyzer results of front-end H-bridge with hybrid CCM-CRM operated buck-based APB converter connected at DC-port, (a) Grid voltage and grid-current waveforms, (b) Grid current harmonic spectrum upto 50 th order, (c) Efficiency drop comparison of selected design operating with CCM, CrCM, and hybrid CCM-CRM.	80
6.1	Bidirectional Active Power Decoupling Converter and single-phase grid-connected AC-DC Converter	84
6.2	Decoupling inductor current, switch currents along with switch voltages and gating signals of APB converter operating with (a) constant-frequency based CCM, (b) variable-frequency based CRM	85
6.3	Hard-switching and Soft-switching regions for different output voltages for SiC MOSFET	87
6.4	Surface Plot of switching frequency, output power and grid frequency with const- raints on f_{sw} (a) at different values of decoupling inductor ($L_b= 40\mu F$, $80\mu F$ and $160\mu F$), (b) at different values of average DC-port voltage and decoupling voltage, (c) at different values of average decoupling voltages and fixed DC-port voltage	88
6.5	Conventional control of (a) APB Converter, (b) front-end AC-DC Converter	89
6.6	Active Ripple Elimination based CRM control for APB converter	91

6.7	Bode diagram of decoupling voltage loop for (a) conventional control with fixed K_{pv} and varying τ_v , (b) conventional control with varying K_{pv} and fixed τ_v (c) proposed control with fixed K_{pv} and varying τ_v . (d) Bode diagram of open-loop decoupling current gain	93
6.8	MATLAB/ Simulink model of buck-based APB converter operating with presented active ripple elimination control and variable frequency-based CRM technique.	95
6.9	Simulation dynamic results with V_b^* change at position ① and load change at ② with (a) conventional control and (b) proposed control	96
6.10	Experimental steady-state results of CCM operated APB converter with hard- switching	98
6.11	(a) Experimental steady-state results of CRM operated APB converter, (b) variation of switching frequency w.r.t average i_b , (b) Soft-switching of both M_1 ($i_b > 0$) & M_2 ($i_b < 0$)	98
6.12	Experimental dynamic response of CRM operated APB Converter without active-ripple elimination ($K_{pv} = 0.05$, $\tau_v = 75ms$): (a) during two V_b^* increments, (b) zoomed -view of V_b^* increase at position ① and ②, (c) during V_b^* decrement. Experimental dynamic response of CRM operated APB Converter without active-ripple elimination ($K_{pv} = 0.05$, $\tau_v = 50ms$): (d) during two V_b^* increments, (e) zoomed-view of V_b^* increase at position ① and ②, (f) during V_b^* decrement. Experimental dynamic response of CRM operated APB Converter with active-ripple elimination($K_{pv} = 0.1$, $\tau_v = 5ms$): (g) during two V_b^* increments, (h) zoomed-view of V_b^* increase at position ① and ②, (i) during V_b^* decrement	99
6.13	Experimental dynamic response of CRM operated APB Converter without active-ripple elimination: (a) during two load increments, (b) zoomed-view of load increase at position ① and ②, (c) during load decrement. Experimental dynamic response of CRM operated APB Converter with active-ripple elimination: (d) during two load increments, (e) zoomed-view of load increase at position ① and ②, (f) during load decrement.	100
7.1	Interleaved half-bridge based on-board integrated electric vehicle charger for single-phase AC to DC power conversion	103
7.2	(a) Presented on-board integrated EV charger with decoupling capability (b) Equivalent circuit diagram of integrated APB-based OBIEV in charging mode	106
7.3	Variation of L_q and L_d at different values of winding currents	110
7.4	Flux density distribution plots at the positive peak value of winding current at rotor angle is (a) 3.75° , (b) 7.5° , (c) 11.25° , (d) 15° , (e) 18.75° , (f) 22.5°	112
7.5	Overall control diagram of OBIEV charger in charging mode	113
7.6	Bode diagrams of G_{vii} and $G_{vii}^*G_c$ with winding inductance (a) 2.7 mH, (b) 1.2 mH	115
7.7	Modulation strategy with variable frequency PWM approach	117
7.8	MATLAB/ Simulink model integrated APB-based OBIEV with variable inductance due to PMSM along with presented control and variable frequency modulation	118

7.9	Integrated APB-based OBIEV charger's (a) Grid Current and winding currents with constant switching frequency PWM, (b) Grid Current and winding currents with variable switching frequency PWM	119
7.10	Harmonic Spectrum with constant switching frequency PWM of (a) winding current, (b) grid current. Harmonic Spectrum with variable switching frequency PWM of (c) winding current, (d) grid current	119
7.11	Simulation results of presented OBIEV charger under (a) G2V mode of operation, (b) V2G mode of operation	120
7.12	Steady-state results of presented OBIEV charger in G2V mode at rated power.	121
7.13	Power quality analyzer results at half-rated power (G2V): (a) grid voltage and grid current, (b) harmonic spectrum of i_g , (c) i_g, v_g vector diagram. Power quality analyzer results at rated power (G2V): (d) grid voltage and grid current, (e) harmonic spectrum of i_g , (f) i_g, v_g vector diagram.	121
7.14	Steady-state results of presented OBIEV charger in V2G mode at rated power.	122
7.15	Power quality analyzer results at half-rated power (V2G): (a) grid voltage and grid current, (b) harmonic spectrum of i_g , (c) i_g, v_g vector diagram. Power quality analyzer results at rated power (V2G): (d) grid voltage and grid current, (e) i_g harmonic spectrum of i_g , (f) i_g, v_g vector diagram	122
7.16	Dynamic performance of presented OBIEV charger with a step 400W increase in output power	123
8.1	Typical architecture of CHB-based fast EV charging station with split-BES and isolated dc-dc converters [2]	128
8.2	Single conversion chain of presented integrated active power buffer for split-BES CHB converter-based EV charging station	129
8.3	Conceptual-evolution of presented IAPB based conversion chain. (a) Schematic with power flow direction of single-CHB module, (b) Power-flow in LF regime of CHB, (c) Power-flow in LF regime of isolated dc-dc converter, (d) Lower order frequency voltage ripple transfer, (e) Final formulated form of presented IAPB based conversion chain	130
8.4	Modes of operation of IAPB with ssplit-BES connected to grid: (a) Mode-I, (b) Mode-II,(c) Mode-III, and (d) Mode-IV	132
8.5	Gate Pulse, HFIT voltages, & HFIT current in (a) Case-I, (b) Case-III	134
8.6	(a) Variation in p.u power in each individual IAPB converter w.r.t ϕ , (b) 3-plot of p.u power v/s ϕ v/s d_{IAPB}	135
8.7	Gate Pulse, HFIT voltages, & HFIT current (a) Case-II, (b) Case-IV	136
8.8	Variation in p.u power in each individual IAPB converter w.r.t ϕ in (a) Case-II, (b) Case-IV	138
8.9	Overall control diagram of IAPB-based split-BES CHB fast EV charging station	139
8.10	dq-control part of front-end CHB based EV charging station	140
8.11	MATLAB/ Simulink model of CHB-based EV charging system with IAPB as isolated DC-DC converter stage along with control and modulation structure.	142
8.12	Steady-state simulation performance of IAPB-based split-BES CHB fast charging station (a) Mode-1, (b) Mode-2,(c) Mode-3	143

8.13	Dynamic Results of presented IAPB-based conversion chain	144
8.14	(a)-(c) Experimental steady-state results of IAPB-based AC-DC-DC conversion chain in Mode-1, (d)-(f) Power quality analyzer results of of IAPB-based AC-DC-DC conversion chain in Mode-1	145
8.15	(a) IAPB's HFIT primary-side voltage, secondary-side voltage, and leakage inductor current, (b) zoomed-view of v_{wx} , v_{yz} , i_{Lk} in positive half cycle of i_{Lk} i.e., position ① which is Case-I, (c) zoomed-view of v_{wx} , v_{yz} , i_{Lk} in negative half cycle of i_{Lk} i.e., position ② which is Case-III	145
8.16	Experimental steady-state results of (a) AC-DC conversion chain for BES charging in Mode-3, (b) zoomed view of v_d , i_{bes} , v_{bes} , (c) EC voltage and current waveforms and their zoomed view at position ④	146
8.17	(a) Experimental steady-state results of IAPB for DC-DC conversion in Mode-4, (b) zoomed view of voltage/ current of IAPB waveforms in Mode-4	146
9.1	Front-end H-bridge AC-DC converter with DC-port connected series-stacked buffer	149
9.2	Current-sensorless control of SSB with adaptive non-linear observer	154
9.3	MATLAB/ Simulink model of series- Stacked Buffer connected at the DC-port of front-end AC-DC converter and SSB operating with non-linear observer based current sensorless technique	155
9.4	Steady-state results of front-end H-bridge based AC-DC converter with series-stacked buffer performing decoupling operation using adaptive non-linear observer based current-sensorless SSB control	156
9.5	Variation in DC-port voltage reference of of front-end H-bridge based AC-DC converter with connected series-stacked buffer performing decoupling operation using adaptive non-linear observer based current-sensorless SSB control	157
9.6	Performance of SSB converter with and without noise in SSB voltage with random noise added at t=4s	157
9.7	Steady-state results of front-end H-bridge based AC-DC converter without series-stacked buffer	158
9.8	Steady-state results of front-end H-bridge based AC-DC converter with series-stacked buffer performing a decoupling operation using adaptive non-linear observer based current-sensorless SSB control	159
9.9	Grid current THD of AC-DC converter (a) without SSB at DC-port, (b) with SSB at DC-port	160
9.10	Variation in DC-port voltage reference of front-end H-bridge based AC-DC converter with connected series-stacked buffer performing a decoupling operation using adaptive non-linear observer based current-sensorless SSB control (a)-(b) with DC-port reference increase from 380V to 420V, (c)-(d) with DC-port reference decrease from 420V to 380V.	161

List of Tables

4.1	Design parameters for MUT-MPC Control	49
5.1	System Parameters for Simulation and Experimentation	76
6.1	Parameters For Simulation and Experimentation	92
6.2	Conventional Control: Impact with variation in K_{pv} and τ_v	93
6.3	Proposed Control: Impact with variation in τ_v	94
7.1	Comparison of different OBIEV Chargers	105
7.2	Design Parameters of PMSM	110
7.3	Parameters For Simulation and Experimentation	118
8.1	Modes of Operation	131
8.2	ZVS turn-ON condition for switches G_1 - G_4	135
8.3	Simulation and Experimental Parameters	143
9.1	Parameters of SSB	158

ABBREVIATIONS

AC	Alternating Current
ADC	Analog-to-Digital
APB	Active Power Buffer
BES	Battery Energy Storage
BSF	Band Stop Filters
CC	Constant Current
CCM	Continuous Conduction Mode
CEC	California Energy Commission
CHB	Cascaded H-Bridge
CRM	Critical Conduction Mode
CV	Constant Voltage
DAB	Dual Active Bridge
DC	Direct Current
DCM	Discontinuous Current Mode
DHB	Dual Half Bridge
DLFR	Double-Line Frequency Ripple
E-caps	Electrolytic DC-Port Capacitor
EV	Electric Vehicles
EMI	Electromagnetic Interference
GaN	Gallium Nitride
GPIO	General Purpose Input/Output
HF	High Frequency
HFIT	High Frequency Isolation Transformer
HPF	High Pass Filters
IAPB	Integrated Active Power Buffer
IGBT	Insulated Gate Bipolar Transistor
IOBEV	Integrated On-Board EV
LF	Low Frequency
LPF	Low Pass Filters

MMC	Modular-Multilevel Converters
MOSFET	Metal-Oxide-Semiconductor Field Effect Transistor
MPPT	Maximum Power Point Tracking
MPC	Model Predictive Control
MV	Medium-Voltage
MUT-MPC	Modified Unit Template Based Model Predictive Control
PET	Power Electronic Transformers
PI	Proportional Integral
PMSM	Permanent Magnet Synchronous Motor
PR	Proportional Resonant
PV	Solar Photovoltaic
PWM	Pulse Width Modulation
SiC	Silicon-Carbide
SOC	State of Charge
SSB	Series-Stacked Buffers
TCM	Triangular Current Mode
THD	Total Harmonic Distortion
ZCD	Zero-Crossing-Detection
ZVS	Zero Voltage Switching

NOMENCLATURE

C_{DC1}	Split DC-link or DC-port Capacitances
C_{DC2}	Split DC-link or DC-port Capacitances
C_{DC}	DC-link or DC-port Capacitance
C_b	APB converter's Capacitor
C_{oss}	Switch-node equivalent capacitance
ΔV_{dc}	DC-link or DC-port low-frequency voltage variation
d_b	Duty of APB
E_{off}	Turn-off transition energy loss
E_{on}	Turn-on transition energy loss
f_{line}	Line frequency
f_{sw}	Switching frequency
$f_{2\omega}$	Twice-Line frequency
$f_{loss(\chi)_N}$	Normalized loss function w.r.t variable χ
$f_{volume(\chi)_N}$	Normalized volume function w.r.t variable χ
H	Magnetic field intensity
h_{t,C_b}	Height of APB Capacitor
h_{t,L_b}	Height of APB inductor
I_{th}	Thresh-hold current
i_b	APB converter's Inductor Current
$i_{b,HF}$	High-frequency triangular component in i_b
$i_{b,LF}$	Twice-line frequency sinusoidal component in i_b
$i_{b,max}$	Maximum i_b for soft-switching
$i_{b,min}$	Minimum i_b for soft-switching
i_{ga}, i_{gb}, i_{gc}	Three-phase Grid Currents
i_g	Single-phase Grid Current
i_o	Output Load Current
l_e	Magnetic path length
L_b	APB converter's Inductor
L_{dd}	Self inductances in PMSM
L_{ga}, L_{gb}, L_{gc}	Interfacing Inductors in Three-phase system
L_g	Grid interfacing Inductor

L_{lk}	Leakage Inductor in isolated DC-DC converter
L_{qd}	Mutual inductance in PMSM
L_{qq}	Self inductances in PMSM
N_{C_b}	Number of parallel APB capacitors
p	Number of poles in PMSM
P_{BES}	Power flowing through each split-Battery Energy Storage
$P_{C,DC1}$	Power in split- DC-link or DC-port Capacitors
$P_{C,DC2}$	Power in split- DC-link or DC-port Capacitors
P_{gL}	Grid interfacing Inductor Power
P_{max}	Maximum output power
P_o	Output Power
$P_{o,i}$	Output power $i = \{20\%, 40\%, 60\%, 80\%, 100\%\}P_{max}$
$P_{Tloss,i}$	Total Loss at i^{th} power level
ϕ	Phase-difference between pulses in isolated DC-DC converter
ψ_d	Flux linkage in PMSM
Q_{max}	Total charge to be removed when $i_b < 0$
Q_{min}	Total charge to be removed when $i_b > 0$
$R_{ds,ON}$	SiC MOSFET's ON-state resistance
S_b	Apparent power
T_{dt}	Dead-time between switches M_1 & M_2
τ_e	Torque developed in PMSM
θ	Temperature dependency factor of $R_{ds,ON}$
V_{dc}	DC-link or DC-port Voltage
V_{dc1}, V_{dc2}	Split DC-link or DC-port Voltages
V_{MUT}	Modified Unit-template
V_{UT}	Unit-template
v_b	APB converter's Capacitor Voltage
v_{ga}, v_{gb}, v_{gc}	Three-phase Grid Voltages
v_g	Single-phase Grid Voltage
ω	Grid Frequency in rad/s
ξ	Damping Factor